Effect of pH on the Formation of Amorphous TiO$_2$ Complexes and TiO$_2$ Anatase during Pyrolysis of TiCl$_4$ Aqueous Solution

Mai Van Tuan [1,2]**, Mai Xuan Dung** [3]**, and Duong Ngoc Huyen** [1,*]

[1] School of Engineering Physics, Hanoi University of Science and Technology, No. 1, Daicoviet, Hanoi, Vietnam; huyen.duongngoc@hust.edu.vn
[2] Department of Natural Sciences, Electric Power University, 235 Hoang Quoc Viet, Hanoi, Viet Nam; tuanmvns@gmail.com
[3] Department of Chemistry, Hanoi Pedagogical University 2, 32 Nguyen Van Linh, Phuc Yen, Vinh Phuc, Viet Nam; xdmai@hpu2.edu.vn
* Correspondence: huyen.duongngoc@hust.edu.vn; Tel.: +84-912 153 128

Abstract: The TiO$_2$ nanostructures resulted by pyrolysis of TiCl$_4$ at low temperature of 80 ^{o}C are found to be a mixture of amorphous TiO$_2$ complexes and anatase nanostructure that depends on the pH of the pyrolysis medium. Anatase nanostructure is predominant at low pH level and gradually converts to amorphous TiO$_2$ complexes with increasing pH level. By means of heat treatment, the TiO$_2$ nanostructures can be recovered from amorphous TiO$_2$ complexes. Amongst of the TiO$_2$ nanostructure recovered from amorphous TiO$_2$ complexes, the anatase nanostructure shows to be the strongest photocatalyst in decomposition of methylene blue.

Keywords: photocatalyst, amorphous TiO$_2$ complexes, TiO$_2$, anatase nanostructure.

1. Introduction

Titanium dioxide (TiO$_2$), a typical metal oxide with high refractive index, chemical stability, long durability, and nontoxicity has been widely used for many applications such as white pigments, textiles, papers, cosmetics, medicines, ceramics, etc. As a *n*-type wide bandgap semiconductor, TiO$_2$ exhibits a unique photoinduced effect that involves photogenerated charge carriers on the material surface that initiate strong redox reaction of adsorbed substances and hydrophilic conversion of itself [1, 2]. The effect offers more potential applications such as splitting hydrogen from water, ultraviolet fillers, photoconductor, photocatalyst, environment cleaning, antibacterial purpose, chemical sensors, dye-sensitized solar cells (DSSC) and so forth [3 - 5].

Under normal condition, TiO$_2$ exists in three main structures: stable rutile, metastable anatase, and brookite phase. For pure phase it is generally accepted that anatase exhibits a higher photocatalytic activity compared to that of rutile despite of its larger band gap (3.2 eV for anatase vs. 3.0 eV for rutile). Longer lifetime for photo-excited electrons and holes in the indirect band gap of TiO$_2$ anatase semiconductor is accounted for the feature [6]. On the other hand, TiO$_2$ in the microstructure have been considered as a poor photocatalyst but in the nanostructured form, due to the quantum confinement the material shows stronger photocatalytic activity when compared to that of the microstructure [7]. The unique photocatalyst of TiO$_2$ nanostructures are size dependent. Therefore, clarification out the synthesis condition to achieve desirable nanostructures of TiO$_2$ is of important to diverse photocatalystic applications.

For the synthesis of TiO$_2$ nanostructure, a variety of techniques based on pyrolysis of Ti precursors such as hydrothermal, solvothermal, sol-gel, direct oxidation, chemical vapor deposition (CVD),

electrodeposition, sonochemical, and microwave method has been used [8]. Pyrolysis offers a simple route to synthesize well-crystalline TiO_2 using inexpensive precursors such as $TiCl_4$, $TiCl_3$, amorphous TiO_2, P_{25}, etc. In addition, the pyrolysis modest medium of low temperature and adjustable time can provide an effective reaction environment for the synthesis of TiO_2 with high purity, good dispersion and controllable crystalline. In a series of experiments made on TiO_2 synthesis in acidic medium, say HCl, we have found that the pyrolysis of $TiCl_4$ results in a nanocrystalline mixture of both the anatase and rutile phase. The TiO_2 anatase mainly suspends in the aqueous solution while the TiO_2 rutile predominantly deposits in the sedimentation [9, 10]. Higher HCl concentration enables the agglomeration of small anatase particles forming uniform cluster and enhances the anatase to rutile transition due to the compensation of Cl^- for the positive charge of polyhedral complexes [9]. In addition to the involvement of Cl^-, the pH level of pyrolysis medium is considered to be a critical parameter regulating the anatase fraction and variety of intermediate type of $Ti(OH)_4$ in the form of $[Ti(OH)_{4-n}(H_2O)_{2+n}]^{n+}$ or Ti-complexes. The Ti-complexes then can decompose into amorphous TiO_2 nanostructure, hence hereafter termed as amorphous TiO_2 complexes. Based on that consumption, in this attempt NH_4OH is used as an additive to adjust pH of the reaction medium and then clarify pH level's effects on the formation of amorphous TiO_2 complexes as well as of anatase nanostructure during pyrolysis of $TiCl_4$ aqueous solution.

2. Results and Discussion

Experiments show that the additive NH_4OH significantly affects the appearance and properties of TiO_2 nanostructures in the resulting materials. As clearly seen in Figure 1, the resulting aqueous solution is transparent at low pH level but gradually changes to slightly opalescent and then separates into transparent and milky parts when the pH level exceeding 2.40. The separated milky part increases with NH_4OH and becomes unchanged as pH level exceeding 7.34. Depending on the transparent or milky state, the surface morphology of the resulting materials transforms from grain to gelation structure as shown in the SEM images in Figure 2. In the sample with pH of 0.98, the resulting material grains are uniform granular with mean size of around 50-70 nm, that in turn has found to be

Figure 1. The appearance of $TiCl_4$ aqueous solution with different pH level after pyrolysis at 80 ºC.

clusters of anatase nanoparticles of 4-5 nm in the mean size [9]. However, when the pH level of the reactive medium increases, the resulting material grain increasingly inflates to coagulated clusters of 150-200 nm in size and gradually become jellylike or amorphous structures as shown in Fig. 2 b to Fig. 2d.
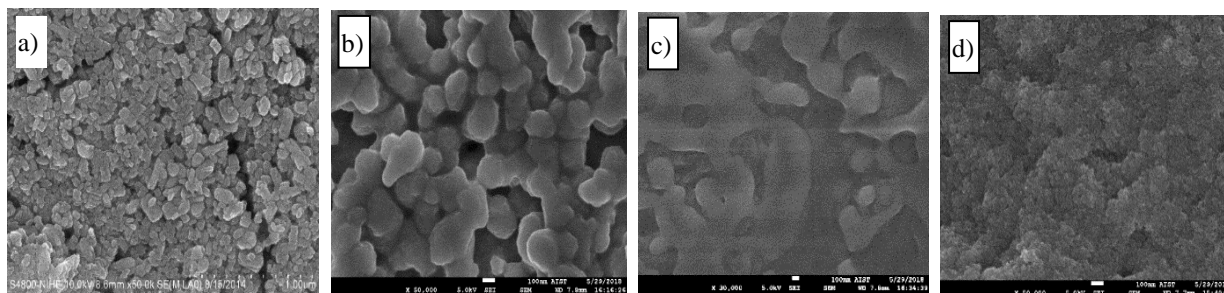
Figure 2. SEM images of TiO₂ resulting from pyrolysis of TiCl₄ in different pH medium at 80 °C: (a) pH = 0.98; (b) pH = 2.45; (c) pH = 10.0 transparent part; (d) pH = 10.0 milky part.

X-ray diffraction spectra in Figure 3 show the evolution of the resulting materials depending on the pH level, i.e, on NH₄OH additive. In the sample with pH level of 0.98, the XRD pattern contains principal peak around 25.29° and the other peaks around 37.80°, 48.05°, 53.89°, 62.68° respectively asigning for the diffraction of anatase structure at (101) and (004), (200), (105), (204) planes (JCPDS no. 00-021-1272). When NH₄OH is added, together with the diffraction peaks from anatase the other sharp diffraction peaks at 22,98°, 32,69°, 40,31°, 46,88°, 52.80°, 58.29°, 68.43° standing for the diffractions at (100), (110), (111), (200), (210), (211), and (220) planes, respectively from NH₄Cl crystal [12]. The disappearance of TiO₂ diffraction in XRD pattern is account for the gradual formation of amorphous TiO₂ or generally amorphous TiO₂ complexes [13]. Using Scherrer equation, i.e., $D = k\lambda/\beta\cos\theta$, where $k = 0.94$, $\lambda = 0.154$ nm and β is FWHM at diffraction angle θ according to (101) peak to calculate the mean size D of anatase particles, it has found that the mean sizes of anatase particle is almost unchanged around 4.5 nm as shown in Table 1. This size is considered to be the limitation of anatase size in the conversion to amorphous TiO₂ complexes.
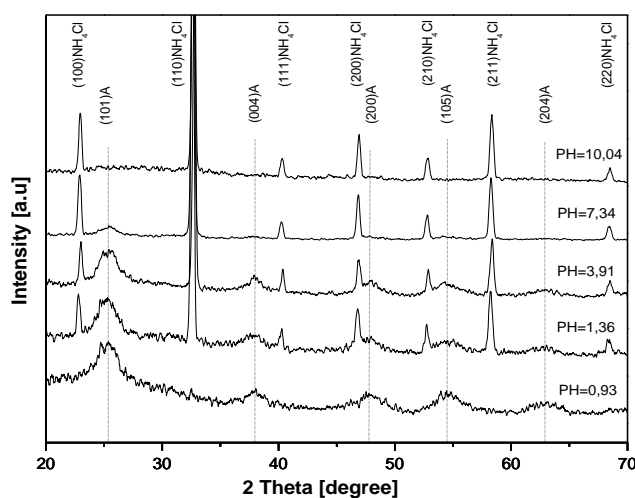
Figure 3. XRD spectra of TiO₂ resulting from pyrolysis of TiCl₄ in different pH medium at 80 °C.

Table.1. The mean size of anatase particle rsulted from pyrolysis of TiCl₄ in different pH medium at 80 °C.

pH	(101) peak FWHM	Size (nm)	Agent addition
0.98	2,007	4,3	No addition
1,36	1,889	4,5	NH₄OH
3,91	1,830	4,7	NH₄OH
7,34	1,888	4,5	NH₄OH
10.04	-	-	NH₄OH

Raman spectra also confirm the present of anatase and NH_4Cl in the resulting materials. As shown in Figure 4, in the starting materials, namely, the sample with pH level of 0,98, the spectrum exhibits vibrational mode around 155 cm^{-1}, 399 cm^{-1}, 513 cm^{-1} and 634 cm^{-1} respectively representing the E_g, B_{1g}, $A_{1g} + B_{1g}$ and E_g modes of anatase structure [14]. The present of NH_4Cl in the gives rise to a broad saddle spectrum of two vibration modes around 168 cm^{-1} and 144 cm^{-1} that is asumed to be the supposition of E_g vibration mode of anatase and ν_2, ν_3 and ν_4 vibration modes of NH_4Cl oscilating against Cl along [100] direction and oscilating along three orthogonal directions [15].
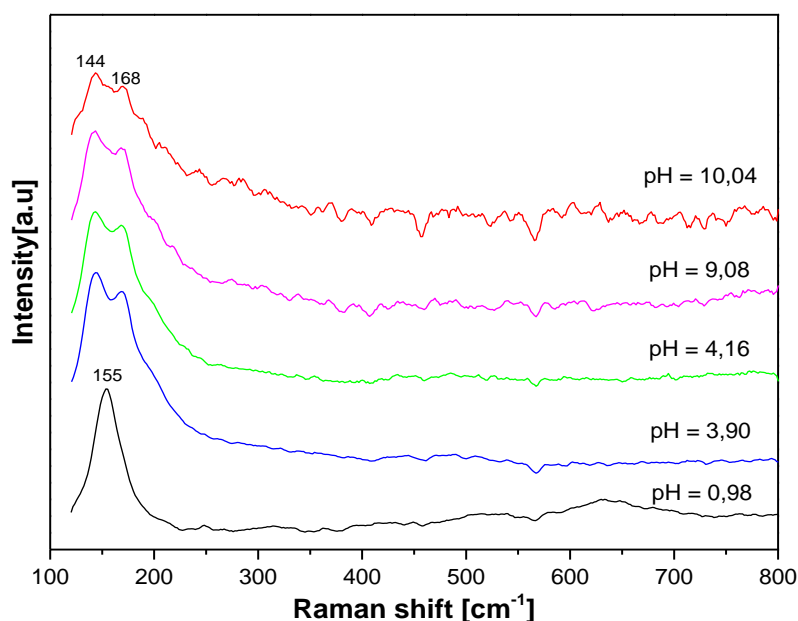
Figure 4. Raman spectra of TiO_2 resulting from pyrolysis of $TiCl_4$ in different pH medium at 80 °C.

a)   b)
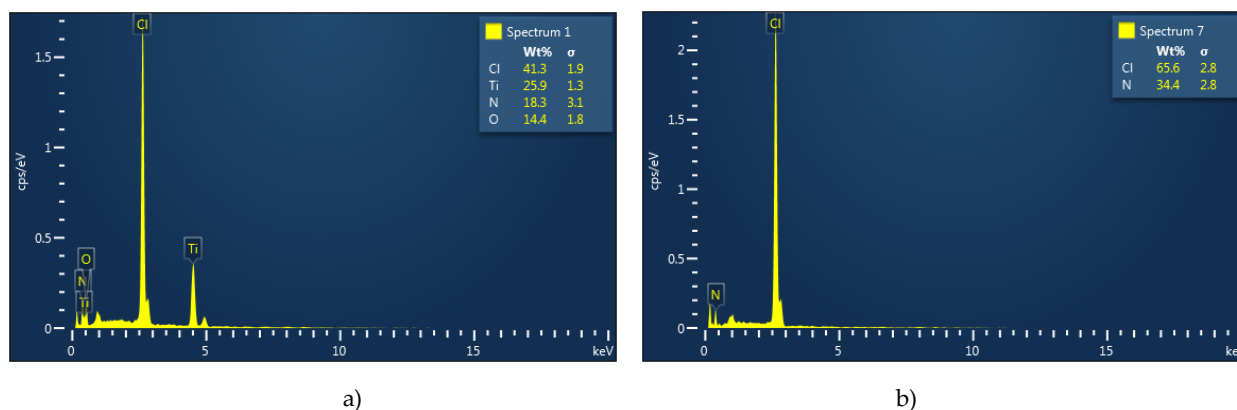
Figure 5. EDS spectra of sample extracted from the milky a) and transparent b) part extracted from pyrolysis of $TiCl_4$ in a medium with pH = 10.04.

The appearance of transparent, opalescent and separable milky part in the solution is believed to be due to the forming and increasing of amorphous TiO_2 or intermediate complexes ($[Ti(OH)_{4-n}(H_2O)_{2+n}]^{n+}$) in the pyrolysis medium. At low pH level, in the acidic aqueous medium with higher concentration of hydrogen ions the formation of amorphous TiO_2 complexes is negligible, the resulting materials is crystallized in the form of grain structure with sharp boundary. With increasing pH level, the acidity of the pyrolysis medium decreases while its base increases. With the hydroxide ion increasing the amorphous TiO_2 complexes is gradually emerged while the grain structure is gradually disappeared. Consequently, with the increase in NH_4OH additive, the separated milky fraction in the medium is gradually increased accompanying with the gradual decrease of anatase

diffraction in the XRD spectra. When the pH level exceeding 7.34, the milky part is unchnged, in the transparent part no trace of Ti present but in the milky as shown in the EDS spectra in Figure 5. This indirectly indicates the fact that the milky trace is an indicator of amorphous TiO_2 complexes and the anatase fraction is completely converted into amorphous TiO_2 complexes at the pH level of 7.34. Due to the armophous nature, no diffraction partten of amorphous TiO_2 complexes is observed in XRD spectra.
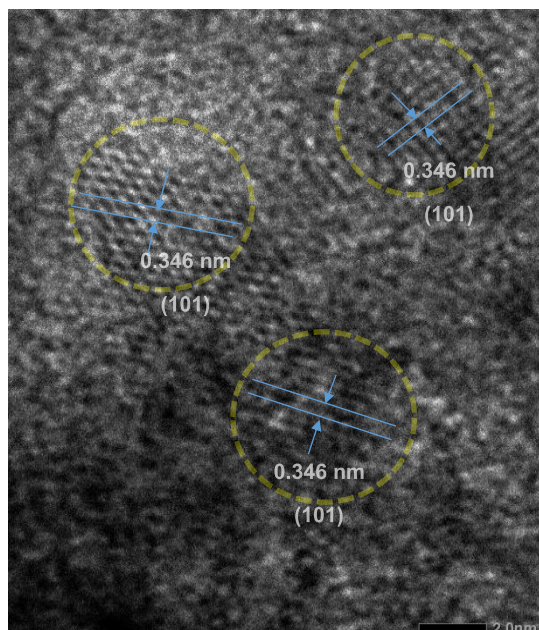
Figure 6. The appearance of anatase nanoparticle scatteringly embedded in the amorphous TiO_2 complexes.

HRTEM image taken from milky sample with pH level of 10.0 as in Figure 6 shows the appearance of tiny nanocrystallites scatteringly embedded in amorphous medium. A lattice spacing of the tiny nanocrystallite around 0.346 nm is identical as the lattice spacing of the (101) plane of TiO_2 anatase. The amorphous surrounding materials is considered to be amorphous TiO_2 complexes. The estimated sizes of TiO_2 anatase particle are the same as of those calculated from XRD pattern, around 4.5 nm that is considered to be the size limitation of anatasse in equilibrium with amorphous TiO_2 complexes. The present of anatase nanoparticles embedded in the amorphous TiO_2 complexes is accounted for the appearance of E_g vibration mode of anatase in Raman spectra in Figure 4.
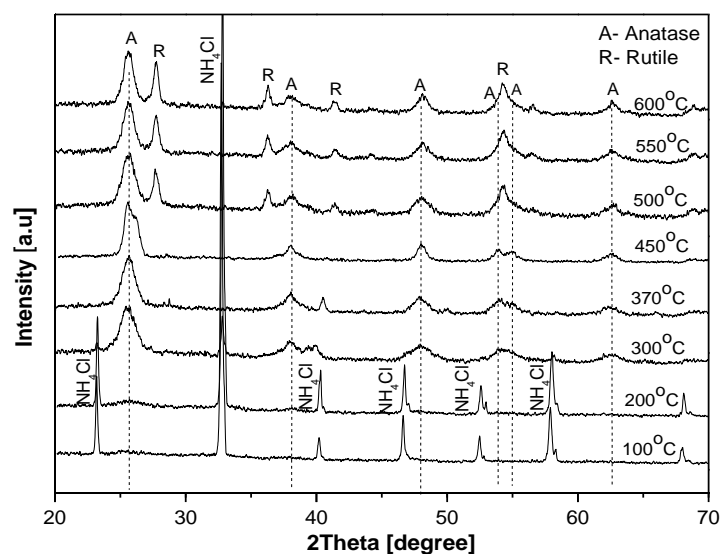
Figure 7. XRD spectra of TiO_2 that resulted from pyrolysis of $TiCl_4$ in the medium with pH =10.04 at 80 °C and then are treated in different elevated temperature.

Under heat treatment at elevated temperature, the XRD and Raman spectra indicate the conversion process from amorphous TiO_2 complexes to anatase and then the transition from anatase to rutile. At heating temperature bellow 200 °C, the XRD pattern in Figure 7 shows only the trace of NH_4Cl but not amorphous TiO_2 complexes nor anatase. However, when heating temperature exceeds 200 °C the anatase diffraction is gradually emerging while NH_4Cl diffraction is gradually disappearing in the XRD patterns. At high temperature, the NH_4Cl is decomposed and vaporized in the form of NH_3 and HCl gases while the amorphous TiO_2 complexes is partly decomposed and recrystallized in the form of TiO_2 anatase. When the heating temperature exceeds 300 °C, the NH_4Cl is completely decomposed the materials is totally converted into TiO_2 nanostructure with predominant anatase. When the heating temperature exceeds 450 °C the appearance of rutile diffraction in the XRD patterns indicates the onset of the anatase-ruttile transition. Using the Scherer equation, we could calculate the mean size of anatase incresing from arouns 4.5 nm at heating temperature of 200 °C to 8.9 nm at heating temperature of 600 °C as shown in Table 2. For the sample with pH level of 0.98, the anatase is predominant over amorphous TiO_2 complexes, the heat treatment is merely the mean to enable the separation of the anatase nanoparticle from the cluster.
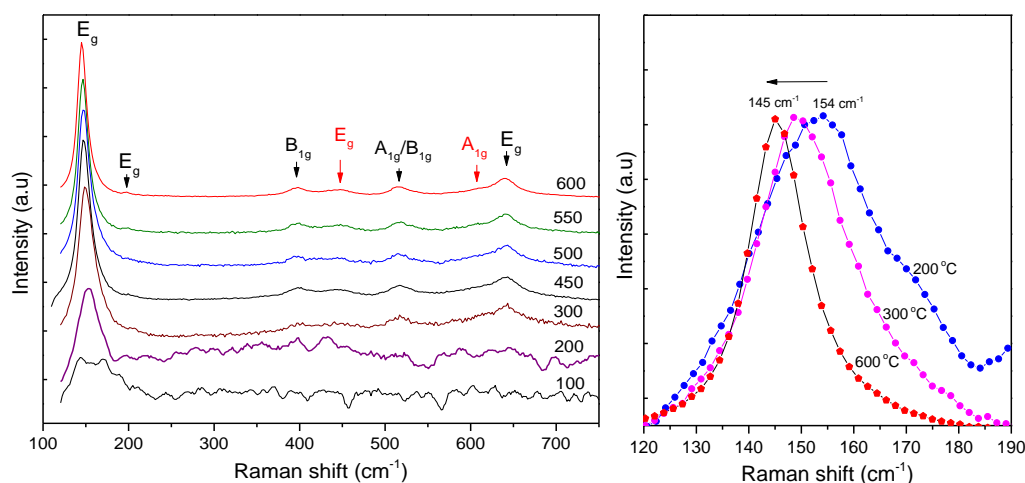
Figure 8. (a) Raman spectra of TiO_2 that resulted from pyrolysis of $TiCl_4$ in the medium with pH = 10.04 at 80 °C and then are treated in different temperature; (b) blue shift of E_g vibration mode as the heating temperature increases from 200 °C to 600 °C.

The Raman spectra also confirm the conversion of anatase from the amorphous TiO_2 complexes (the milky part) when it is heat up as can be seen in Figure 8. With baking temperature bellow 200 °C the Raman spectrum is a composition of NH_4Cl vibration mode centered around 168 cm^{-1} and 144 cm^{-1} and the Eg vibration mode TiO_2 anatase at 147 cm^{-1} [14]. As the heating temperature increases from 200 °C to 600 °C the E_g vibration mode shows a shift in frequency from 154 cm^{-1} to 145 cm^{-1} and an increase in FWHM (see in Table 2). The feature accounts for the increase in size of the TiO_2 nanocrystallites.

The formation of TiO_2 nanostructures by pyrolysis of $TiCl_4$ in elevated pH medium is explained by the decomposition, dissolution mechanism [16]. At elevated temperature exceeding 80 °C, $TiCl_4$ is decomposed into $Ti(OH)_4$ and then into amorphous TiO_2 complexes, TiO_2 anatase and HCl in the pyrolysis medium. The component ratio of TiO_2 anatase and amorphous TiO_2 complexes then is established by an equilibrium between H$^+$, OH$^-$ and Cl$^-$ in the medium. In the acidic medium, TiO_2 predominantly exists in the form of tiny anatase crystallites whose mean size bellow the size limitation for the anatase to rutile transition [9, 10]. On the other hand, the weaker acidic, stronger basic medium enhances the formation of $Ti(OH)_4$ and then amorphous TiO_2 complexes. By addition of NH_4OH to reduce the activity of HCl and increase of basic level in the reaction medium, the anatase portion is decreased and the amorphous TiO_2 complexes are increased in the medium. At low pH level, anatase fraction is dominant while at high pH level the amorphous TiO_2 complexes is dominant.

The amorphous TiO_2 complexes can be converted back to the TiO_2 anatase nanoparticles by heat treatment at temperature around 300 °C.

Table.2. The mean size and Eg vibration mode of anatase resulting from annealing amorphous TiO_2 complexes.

Baking temp.	Crystallite size (nm)	E_g mode peak (cm^{-1})	FWHM of E_g mode (cm^{-1})
200°C	4.5	154	31
300°C	6.2	150	25.8
450°C	6.8	148	18.9
500°C	6.8	148	18.1
550°C	8.3	147	15.9
600°C	8.9	145	14.5

Experiments show that amorphous TiO_2 complexes and anatase nanoparticles exhibit strong photocatalytic activity upon exposure to UV light radiation. Quatitatively, a mixture of 50 *ml* of 0.25 *μmol* methylene blue (MB) aqueous solution and 50. 0 *mg* of amorphous TiO_2 complexes or TiO_2 anatase nanoparticles is stirred magnetically under dark conditions for 30 min before exposed upon a UV mercury vapor lamp. After a fixed exposure duration, 1.0 *ml* of the aqueous solution is taken out for UV-Vis characterization. The percentage of MB left in the solution standing for the photocatalytic activity of amorphous TiO_2 complexes or TiO_2 anatase nanoparticles is calculated by comparison of the relative intensity of MB principal adsorption peak in the UV-Vis spectrum. As shown in Figure 9, the photocatalytic activity of the materials is affected by synthesis condition, i.e, pH level of synthesized medium and the heat treatment following. The rates of photocatalytic oxidation of MB over UV illuminated TiO_2 show to be well fitted to the Langmuir–Hinshelwood (L-H) kinetics model [17] as seen in the plots.
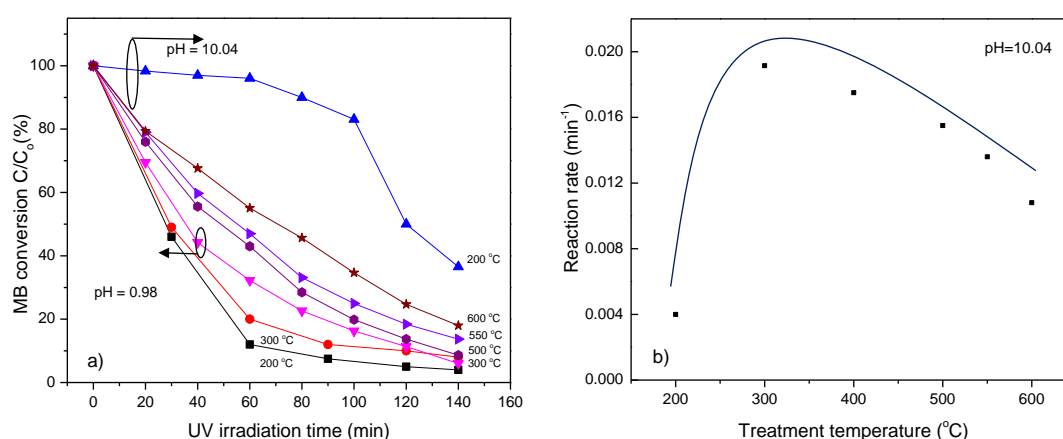
Figure 9.   a) Photocatalytic activity of TiO_2 synthesized in acidic (pH = 0.98) and basic (pH =10.04) medium . b) Photocatalytic activity of amorphous TiO_2 complexes depends on annealing temperature.

When MB concentration is small the L-H equation can be simplified to an apparent first-order: $ln(C_0/C_t) = kt$ or $C_t = C_0\ exp\ (-kt)$, where C_0 is the initial concentration of MB, C_t is the concentration of the MB at illumination time t, k is a constant standing for the photoctalitic redox or reaction rate. By fitting the MB decomposition curve in Figure 9 a) to the L-H equation the dependence of the reaction rate on the treatment temperature is shown in Figure 9 b). The reason is accounted for the Ti complexes, NH_4Cl, TiO_2 anatase and ruttile content in the materials. With respect to the predominant amorphous TiO_2 complexes synthesized in the medium with pH = 10.04, the photocatalysis (reaction

rate) of the materials is weak as heating temperature bellow ~200 °C but rapid increases with elevated temperature beond that point. The anatase appears in the materials is accounted for the decomposion of amorphous TiO_2 complexes and then recrystallization. At heating temperature around 300 °C, NH_4Cl and amorphous TiO_2 complexes are totally decomposed the materials completely turn into pure anatase as a result the photocatalytic activity of the materials is found to be maximum. Futher increasing the heat temperature, the photocatalytic is reduced due to the growth in size of anatase particle and the appearance rutile fraction from the anatase-rutile transition. As a comparison with the sample of predominant anatase that is synthesized in the medium of pH = 0.98, a lower heating temperature of around 200 °C is adequate to completely convert the materials to totally pure anatase.

3. Materials and Methods

Titanium tetrachloride ($TiCl_4$) of 99.9 % purity (Sigma Aldrich Chemical Co.) as Ti precursor was used as received. Ammonium hydroxide solution (NH_4OH) of 28 % NH_3 (Merck Corp.,) was used as basic agent to change the pH of pyrolysis medium. The TiO_2 synthesis process was straightforward as follows: $TiCl_4$ was added dropwise into DI water at 5 **°C** to a concentration of 0.04 M, the pH level of the solution then was dropped to around 0.98 (starting point). By adding a small amount of NH_4OH into the solution the pH level was adjusted and preserved at a point in range of 0.98 to 10.04. The solution then was poured into test tubes and placed in an oven at 80 **°C**, the onset point of $TiCl_4$ decomposition. The solution was gradually changed to opalescent suspension indicating that the $TiCl_4$ was thermally decomposed and converted into Ti complexes $[Ti(OH)_{4-n}(H_2O)_{2+n}]^{n+}$ (n is number of protonated OH^- groups) and then TiO_2 accompanying with the formation of HCl and NH_4Cl [11]. The pyrolysis was carried on about 3.0 h and the power was shut down, the solution was slowly cooled to room temperature. Depending on pH level, the appearance of resulting solution shows either transparent, opalescent or clearly splits into transparent and milky part as seen in Figure 1. For characterization, these parts were separated and dried by vacuum evaporation then were thermally treated in an oven with baking temperature up to 600 °C.

The structure of the resulting materials was determined by D8 Advance Bruker diffractometer using CuK_α radiation of 0.154 *nm* wavelength. The mean size, D of TiO_2 crystallites was calculated using Scherrer equation, i.e., $D = k\lambda/\beta cos\theta$, where k = 0.94, λ = 0.154 *nm* and β is full width at half maximum (FWHM) according to the principal diffracted angle θ, i.e., (101) peak for anatase. Raman spectra were obtained on a LabRAM HR800 (Horiba) using a 632.8 nm excitation laser at a resolution of 1.0 cm^{-1}. TEM images were obtained using a JEOL JEM-2100 Transmission Electron Microscope. SEM images were conducted on a JEOL JEM-7600F Field Emission Scanning Electron Microscope. The photocatalystic activity of TiO_2 nanostrutures was determined by measuring the degradation rate of methylene blue (MB) under UV light radiation.

4. Conclusion

The pyrolysis of $TiCl_4$ aqueous solution generally results in a mixture of TiO_2 anatase nanostructure and amorphous TiO_2 complexes. The ratio of TiO_2 anatase nanostructure and amorphous TiO_2 complexes can be controlled by changing the pH of the pyrolysis medium. The anatase fraction is predominant at low pH level and gradually declines and completely converts to the amorphous TiO_2 complexes at high pH level. By addition of NH_4OH to adjust the pH, the pyrolysis of a 0.04M $TiCl_4$ aqueous solution results in a mixture of TiO_2 anatase nanostructure and amorphous TiO_2 complexes at pH bellow 7.34 and predominant amorphous TiO_2 beyond that point.

The amorphous TiO_2 complexes is found to be converted to TiO_2 nanostructure by heat treatment. With annealing temperature around 300 **°C**, the amorphous TiO_2 is completely converted into anatase nanostructure and gradually transform into rutile at high temperature. Amongst of the TiO_2 nanostructure recovered from amorphous TiO_2 complexes, the anatase nanostructure shows to be the strongest photocatalyst in decomposition of methylene blue.

Acknowledgments: The authors gratefully acknowledge financial support received in the form of a Basic Research Project Grant in Aid (T2008-PC-123) provided by Hanoi University of Science and Technology (HUST), Vietnam.

Conflicts of Interest: The authors declare no conflict of interest.

References

1. Ulrike Diebold, The surface science of titanium dioxide, Surf. Sci. Rep. **2003**, 48, pp.53-229.

2. K. Hashimoto, H. Irie, and A. Fujishima, TiO_2 photocatalysis: a historical overview and future prospects, Jpn. J. Appl. Phys. **2005**, vol. 44 (12), pp. 8269–8285.

3. K. Nakata and A. Fujishima, TiO_2 photocatalysis: design and applications, J. Photochem. Photobiol. C **2012**, vol. 13 (3), pp. 169–189.

4. M. Montazer, S. Seifollahzadeh, Enhanced self-cleaning, antibacterial and UV protection properties of nano TiO_2 treated textile through enzymatic pretreatment. Photochem Photobiol. **2011**, 87, pp. 877–883.

5. A. Fujishima and K. Honda, Electrochemical photolysis of water at a semiconductor electrode, Nature **1972**, vol. 238 (5358), pp. 37–38.

6. L. Liu, H. Zhao, J. M. Andino & Y. Li, Photocatalytic CO_2 reduction with H_2O on TiO_2 nanocrystals: Comparison of anatase, rutile, and brookite polymorphs and exploration of surface chemistry. ACS Catal. **2012**, 2, pp. 1817–1828.

7. S. M. Gupta and M. Tripathi, A review of TiO_2 nanoparticles, Chinese Sci. Bull. **2011**, vol. 56 (16), pp. 1639–1657.

8. M. M. Byranvand, A. Nemati Kharat, L. Fatholahi, and Z. Malekshahi Beiranvand, A review on synthesis of nano-TiO_2 via different methods, J. Nanostruct., **2013**, vol. 3, pp. 1–9.

9. N. T. Tung, D. Ng. Huyen, Effect of HCl on the Formation of TiO_2 Nanocrystallites, J. Nanomater. **2016**, vol. 2016, Article ID 6547271.

10. N. T. Tung, M. X. Dung and D. Ng. Huyen, Simultaneous Synthesis of Anatase Colloidal and Multiple-branched Rutile TiO_2 Nanostructures, B. Korean Chem. Soc., **2017**, 38(3); p. 401-405.

11. Q. Zhang, L. Gao, Langmuir **2003**, 19, 967.; V. Jordan, U. Javornik, J. Plavec, A. Podgornik, A.Recnik, Sci. Rep. **2016**, 6, 24216.

12. Downs, R. T., Bartelmehs, K. L., Gibbs, G. V., & Boisen, M. B., Interactive software for calculating and displaying X-ray or neutron powder diffractometer patterns of crystalline materials. Am. Mineral., **1993**, 78(9-10), pp. 1104-1107.

13. Mónica Andrea Vargas, Jorge E. Rodríguez-Páez, Amorphous TiO_2 nanoparticles: Synthesis and antibacterial capacity, J. Non-Cryst Solids **2017**, 459, pp. 192–205.

14. M.N. Iliev, V.G. Hadjiev, A.P. Litvinchuk, Raman and infrared spectra of brookite (TiO_2): Experiment and theory, Vib. Spectrosc., **2013**, 64, pp. 148–152.

15. R. S. Krishnan, Raman spectrum of ammonium chloride and its variation with temperature, Proceedings of the Indian Academy of Sciences, Section A, 26 (6) (1947) 432-449.

16. S. Dai, Y. Wu, T. Sakai, Z. Du, H. Sakai, and M. Abe, Preparation of highly crystalline TiO_2 nanostructures by acid-assisted hydrothermal treatment of hexagonal-structured nanocrystalline titania/cetyltrimethy-ammonium bromide nanoskeleton, Nanoscale Res. Lett. **2010**, vol. 5(11), pp. 1829–1835,

17. G. W. Roberts and C. N. Satterfield, Effectiveness Factor for Porous Catalysts. Langmuir-Hinshelwood Kinetic Expressions, Ind. Eng. Chem. Fundamen., **1965**, 4, 3, pp. 288–293.